Validation of European-scale simulated wind speed and wind generation time series

Murcia, Juan Pablo; Koivisto, Matti Juhani; Luzia, Graziela; Olsen, Bjarke T.; Hahmann, Andrea N.; Sørensen, Poul Ejnar; Als, Magnus

Published in:
Applied Energy

Link to article, DOI:
10.1016/j.apenergy.2021.117794

Publication date:
2022

Document Version
Publisher's PDF, also known as Version of record

Applied Energy 305 (2022) 117794

Contents lists available at ScienceDirect

Applied Energy

journal homepage: www.elsevier.com/locate/apenergy

Validation of European-scale simulated wind speed and wind generation time series

Juan Pablo Murcia *, Matti Juhani Koivisto, Graziela Luzia, Bjarke T. Olsen, Andrea N. Hahmann, Poul Ejnar Sørensen, Magnus Als

Department of Wind Energy, Technical University of Denmark, Roskilde, Denmark

ARTICLE INFO

Keywords:
Large scale energy system
Wind energy
Atmospheric reanalysis
European
Renewable energy
Wind generation
Validation

ABSTRACT

This paper presents a validation of atmospheric reanalysis data sets for simulating onshore wind generation time series for large-scale energy system studies. The three reanalyses are the ERA5, the New European Wind Atlas (NEWA) and DTU's previous generation European-level atmospheric reanalysis (EIWR). An optional scaling is applied to match the microscale mean wind speeds reported in the Global Wind Atlas version 2 (GWA2). This mean wind speed scaling is used to account for the effects of terrain on the wind speed distributions. The European wind power fleet for 2015–2018 is simulated, with commissioning of new wind power plants (WPPs) considered for each year. A generic wake model is implemented to include wake losses that are layout agnostic; the wake model captures the expected wake losses as function of wind speed given the technical characteristics of the WPP. We validate both point measurement wind speeds and generation time-series aggregated at the country-level. Wind measurements from 32 tall meteorological masts are used to validate the wind speed, while power production for four years from twelve European countries is used to validate the simulated country-level power production. Various metrics are used to rank the models according to the variables of interest: descriptive statistics, distributions, daily patterns, auto-correlation and spatial-correlation. We find that NEWA outperforms ERA5 and EIWR for the simulated wind speed, but, as expected, no model is able to fully describe the auto-correlation function of the wind speed at a single point. The mean wind speed scaling is found to be necessary to match the distribution of generation on country-level, with NEWA-GWA2 and ERA5-GWA2 showing highest accuracy and precision for simulating large-scale wind generation time-series.

1. Introduction

The generation of electricity from renewable sources is a key component of the climate change mitigation plans worldwide. For the first time in 2019, the renewable power generation grew faster than the electricity demand [1]. But, the global share of renewable electricity generation would need to increase to 28% by 2030 and 66% by 2050, to keep the mean global temperature rise below 2 °C by the end of the century [1]. In the European Union the share of renewable energies reached 32% of electricity generation and a 18% of the total energy consumption in 2018 [2], these shares are planned to grow to 50% of the electricity and 32.5% of the total energy by 2030 [2].

Accurate simulation of wind energy generation time series are needed in energy system design studies, such as the sector coupling and transmission reinforcement designs in Europe [3] and in the North Sea [4], as variability in wind power generation impacts electricity prices, and correlations in generations between countries can impact optimal transmission expansion. Long time series (tens of years) are needed for system adequacy analyses [5]. Modeling temporal dependencies in wind generation is important, e.g., when analyzing the behavior of wind generation ramps in power system integration studies [6]. Regional aggregated wind generation time series can be obtained using a reanalysis data set in two approaches: (1) a bottom-up modeling of the details of each plant [7], i.e. installed capacity, location, wind turbine type, hub height, rotor diameter, etc. (2) a top-down approach that relies on historical generation observations and calibration of transfer functions to be applied to future scenarios [8]. Furthermore bias correction of either the wind speeds or wind generation is usually needed and can be done without the use of measurements, e.x. using the global wind atlas to correct mean wind speeds [7] or based on calibration of wind speed correction to match generation observations [9].

* Corresponding author.
E-mail address: jumu@dtu.dk (J.P. Murcia).

https://doi.org/10.1016/j.apenergy.2021.117794
Received 23 February 2021; Received in revised form 30 August 2021; Accepted 1 September 2021

Nomenclature

u	Wind speed time-series at a location
I	Turbulence intensity
P	Country-level standardized wind generation time-series
P_{WT}	Turbine rated power
N_{WT}	Number of turbines in a plant
D_{WT}	Rotor diameter
A_{WPP}	Land-use area of the plant
y	Variable holder for nomenclature, can be u or P
x	Variable holder for nomenclature, can be either location for u, or country for P
t	Time
Δy	One hour ramps time-series for y: $\Delta y = y(t+1) - y(t)$
$\overline{y}$	Long-term mean of y, averaged over time for the full period available
$\overline{y}_{MD}$	Mean of y at each month and each hour of the day
e	All errors are computed between a model and observations
$e_{\overline{y}}$	Error in long-term mean y
$e_{\overline{y}\,MD}$	Error in normalized monthly-hourly mean y
$e_{F\,y}$	Area between the model and observed empirical cumulative density functions
MAE_y	Mean absolute error
RMSE_y	Squared root of the mean squared error
r_y	Sample (or prediction) correlation coefficient
$\rho(y_1, y_2)$	Correlation coefficient (Pearson's) between two time series
e_{y_1}	Error in 1h lag auto-correlation in y
$e_{y\,N_t}$	Mean error in the N_t hours lag auto-correlations in y
e_{X_y}	Mean error in the spatial-correlation of y, i.e. correlation between time-series at different locations
$e_{X_{\Delta y}}$	Mean error in the spatial-correlation of the one hour ramps of y, i.e. correlation between ramp time-series at different locations
WT	Wind turbine
WPP	Wind power plant

Validation of mean wind speed or predictions of annual energy production for synthetic wind turbines was carried out in several studies [10]. For energy system modeling, predicting the correct mean wind speed or annual energy production is not enough, as it requires the simulation of time series with the right distribution (probability density function, PDF), auto-correlation and spatial-correlation among the different locations. Individual reanalysis data sets have been validated before for MERRA and MERRA-2 [9], for MERRA with micro-scale wind speed scaling from the Global Wind Atlas (GWA) [11], for ERA-Interim with WRF dynamic scaling and GWA micro-scale wind speed scaling [7]. The ERA5 reanalysis was shown to give more accurate wind generation predictions in comparison to MERRA-2 [12]. Recently, a validation study of multiple weather data sets in France was published by [13] and it concluded that (1) high resolution regional reanalysis (COSMO-REA2) or high resolution weather models (AROME) tend to have lower prediction errors, (2) ERA5 is very skilled in prediction of regional wind generation despite its lower resolution and biases in mean wind speed predictions in mountainous locations, and (3) NEWA and MERRA-2 show problems with the diurnal cycle that translates into larger biases in mean wind speed. New generation regional reanalyses such as COSMO-REA2 have been shown to better correlate to both wind speed measurements [14] and wind generation in France [13] and in Switzerland [15]

The purpose of this paper is to assess the accuracy of several reanalysis data sets for wind generation simulations in large scale scenarios. Two validations data sets are presented in this paper: (1) several years of measurements from 32 met masts and (2) reported country-level wind energy generation for four years. Validation metrics are defined for several variables of interest, and the models are ranked according to each metric. Validation metrics are defined in terms of prediction errors of descriptive statistics, mean daily cycle, auto-correlation, spatial-correlation, and the cumulative density function distance.

The hypothesis of this study is that it is possible to accurately simulate the large-scale regional wind energy generation using the global reanalysis ERA5 corrected with microscale wind speed effects with the same accuracy as with time series from detailed mesoscale reanalysis simulations. Mesoscale models are expected to show higher accuracy for modeling individual sites.

This paper presents a new optic of the validation of reanalysis data focused on the specific need of large-scale wind generation simulations, and compares multiple weather data sets including microscale downscaling in European level. Compared to previous works where bias correction of wind speeds was done based on measured generation data per country [9] or as a global wind speed correction factor to better match capacity factors [12], in this paper downscaling is based on microscale wind speed data (Global Wind Atlas, GWA). Measured power generation is not used as part of the model calibration, which allows model validation in the power generation domain to be fully independent of the measured generation data. A more detailed wake loss model differentiates this study from [11]. When microscale effects and wake losses are considered, the resulting power generation times series show strong agreement with measured data, which indicates that measured generation data is not required in the model calibration; and in general shows improved modeling results than applying wind speed corrections such as [16]. Compared to [10], this paper adds the comparison of spatio-temporal dependencies in wind time series.

Section 2 describes the reanalysis data sets and the measurements evaluated in this paper. Sections 3 and 4 presents the modeling methods and the validation metrics. Section 5 presents the results for the two validation cases. Sections 6 and 7 discuss and conclude the paper.

2. Data

2.1. Reanalysis data sets

Data from three atmospheric reanalysis are compared: ERA5 [17], DTU's previous generation European level weather reanalysis simulation performed using the Weather Research and Forecasting (WRF) model [18] and the New European Wind Atlas (NEWA) [19]. Additionally, a mean wind speed scaling is applied to each reanalysis data set to match the mean wind speed reported by the Global Wind Atlas v2 (GWA2) micro-scale resource assessment, see Section 3.2 for details on this scaling. Resolutions and periods of availability for each data set are presented in Table 1.

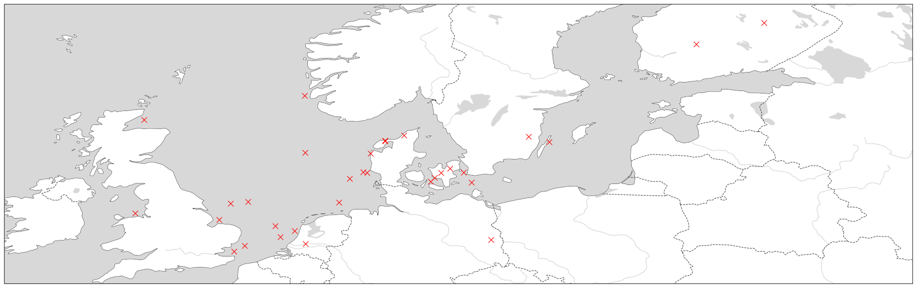

Fig. 1. Locations of the wind speed measurements.

Table 1
Description of the reanalysis data sets. *Wind speed were interpolated from the model levels to model height above ground level.

	ERA5	NEWA	EIWR	GWA2
Institution	ECMWF	DTU	DTU	DTU
References	[17]	[10]	[18,20]	[7]
Model	IFS Cy41r2	WRF	WRF	WAsP
Boundary conditions	–	ERA5	ERA-Interim	–
Spatial coverage	Global	Europe	Europe	Global
Horizontal grid spacing	0.25° ≈ 30 km	3 km	3 km	250 m
Vertical levels	[10 25 50 75 100 150 200 250]*	[50 100 150 200]	[50 80 100 120 150]	[50 100]
Time coverage	1979–2018	2006–2018	1982–2018	–
Time resolution	1 h	30 min	1 h	–

2.2. Wind speed measurements

Data from 32 sites were collected from different sources and processed, see Table B.9. Time series of wind speed measured at the level closest to 100 m height, originally at 10 min averaged resolution, were aggregated to hourly resolution. Gaps are identified and discarded from the models in the validations. All data sets were subjected to an adapted version of the quality control routine described in [21] and a rough attempt was made to minimize the effect of flow distortion caused by the mast on the wind speed measurements. The observations cover different time periods from 1996 to 2019 with at least one full year, see Table B.9. The locations of the masts are shown in Fig. 1.

2.3. European wind energy fleet

We use the database of wind plant installations in Europe from [22]. This database includes locations, hub height, installed capacity, commissioning year and turbine type among other parameters for each wind power plant in Europe. Additionally, the database includes the power curves for most turbine manufacturers and turbine models. Individual installation scenarios are run for each production year within [2015–2018], the plants expected to be operating are selected accordingly to the commissioning year, and an assumed plant lifetime of 25 years. Plants within 2 km of each other are merged into a single plant to consider the plant-to-plant wake losses. As the WPP data set sometimes reports even single turbines as plants, this merging gives a more unified specification of WPP sizes across Europe. Plant-to-plant wakes are in particular important for countries in Central and Western Europe where plants (and individual turbines) are sited in close proximity to each other. In this study three different wind turbine spacings were used: 6 rotor diameters for the Nordic countries, 3 rotor diameters for Germany and France, and 10 rotor diameters for South European countries. The difference in WT spacing follows the trends on installation density in Germany presented in [23]. An overview of the country level aggregated WPP characteristics is given in Table 2 (see Fig. 2).

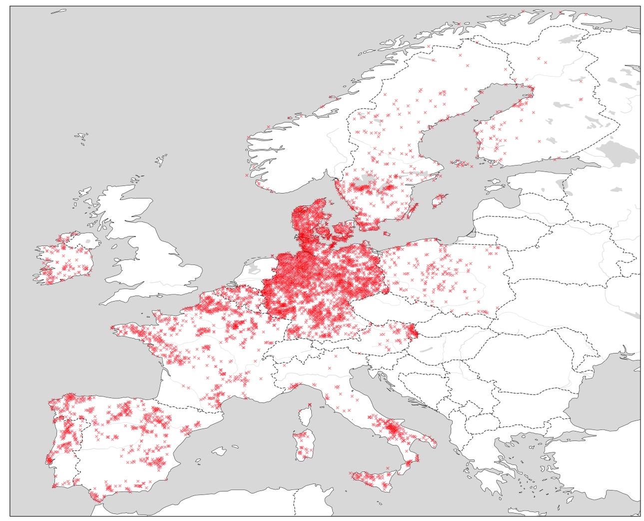

Fig. 2. Location of wind power plants operating in 2018.

2.4. Country-level wind generation measurements

Hourly resolution onshore wind generation data from the ENTSO-E Transparency platform are obtained from [24]. Hourly installed capacity data from [24] for Germany, Denmark and Sweden is used for calculating standardized generation time series for these countries. For the other countries, annual installed onshore wind capacity data from [25] is used with linear interpolation of the annual values to estimate the standardized generation.

A comparison of annual capacity factors from several sources is presented in Table 3. IRENA is calculated using both annual onshore wind generation and installed capacity from [25]. ENTSO-E considers generation from [24] and onshore wind installed capacity directly from [26]. Mean of start-of-year and end-of-year installed capacity is used to approximate the annual installed capacity.

Curtailment is also presented in Table 3 for Germany and Ireland, where data is available from [27] and [28], respectively. For Germany, curtailment shares are available for 2015 and 2016; 2017 and 2018 curtailment are modeled by taking mean of the 2015 and 2016 values. On average for the period 2015–2018, curtailment share of 4.8% is found for Germany, and 4.2% for Ireland. As curtailment data is available only on annual level, it is not applied on the hourly time series, however, it is reported in this article to show the challenges of finding accurate measured data to validate the large-scale simulations.

The resulting capacity factors in Table 3 show that for some countries, e.g., Austria, Denmark and Italy, the sources give approximately the same capacity factors. However, significant differences can be seen in e.g. Ireland and France. For Germany, standardized generation time series used in this article show much higher capacity factor than the other two sources.

Table 2
Fleet aggregated statistics for wind energy installations for 2018. Weighted average parameters are given with respect to the installed capacity of each plant (wm).

Country	Installed capacity [MW]	WPP number	WT rated power [MW] (wm)	WT diameter (D) [m] (wm)	Hub height [m] (wm)	WT number (wm)	WPP land-use area [km^2] (wm)	WT power density [W m^2] (wm)	Efficiency (wm)	WT spacing [D] (wm)
Austria	2726	117	2.4	89	112	25	1.88	390	0.95	6
Denmark	3449	788	1.7	71	66	7	0.41	390	0.95	6
Finland	1624	88	3.2	119	129	14	1.80	290	0.95	6
France	13008	854	2.2	88	85	11	0.19	370	0.95	3
Germany	52930	3646	2.0	83	102	19	0.28	380	0.95	3
Ireland	3143	139	2.0	78	73	27	1.50	410	0.95	6
Italy	10007	364	1.6	75	71	33	4.26	360	0.95	10
Norway	1116	21	2.6	93	84	35	2.85	390	0.95	6
Poland	4732	193	2.2	92	97	22	1.70	330	0.95	6
Portugal	5279	186	2.1	81	78	33	5.69	410	0.95	10
Spain	20732	573	1.5	72	68	57	7.55	360	0.95	10
Sweden	4660	507	2.2	92	96	18	1.70	330	0.95	6

Table 3
Measured capacity factors (mean of 2015–2018) as reported from different sources and from the measured time series used in this paper. Expected capacity factor without curtailment in brackets.

Country	IRENA	ENTSO-E	$\overline{P}$
Austria	0.24	0.25	0.25
Denmark	0.26	0.26	0.26
Finland	0.31	0.29	0.28
France	0.23	0.20	0.21
Germany	0.20 (0.21)	0.19 (0.20)	0.25 (0.27)
Ireland	0.29 (0.30)	0.38 (0.40)	0.29 (0.30)
Italy	0.21	0.22	0.21
Norway	0.32	0.30	0.30
Poland	0.28	0.25	0.26
Portugal	0.28	0.28	0.27
Spain	0.25	0.24	0.24
Sweden	0.30	0.33	0.32

3. Methods

The overall simulation model chain is depicted in Fig. 3.

3.1. Wind speed interpolation

Cubic-spline interpolation is used for horizontal interpolation of wind speeds. Power law interpolation between the two closest heights available in the reanalysis is used for vertical wind speed interpolation. This approach is equivalent to a piece-wise linear interpolation in log–log scale. Note that the wind speeds are interpolated for every time step, without applying any smoothing or filter.

3.2. Mean wind speed scaling

The long-term mean wind speed maps are pre-computed for every reanalysis data set at the available heights. The mean wind speed from GWA2 is averaged over the land-use area of the plant in order to have a representative wind speed for the full plant and the value at the center point of the plant. The scaling factor is computed between the long-term mean wind speed from the reanalysis and the mean wind speed from the GWA2. Both mean wind speeds are interpolated using the methodology described in 3.1. This methodology was used in several studies such as [7,11,29]. Fig. 4 depicts the scaling factors at the WPP installation locations in 2018.

3.3. Wake modeling

The layout information is not available for any of the plants in this study, therefore a generic wake model was developed to capture the wake losses as a function of the wind speed (u), mean turbulence intensity at the site ($\overline{I}$), turbine rated power (P_{WT}), number of turbines (N_{WT}), rotor diameter (D_{WT}) and area of the plant (A_{WPP}). The long-term mean turbulence intensity over Europe is estimated using NEWA's turbulent kinetic energy.

$$\tilde{\mathbf{WL}} \approx \mathbf{WL}(u, \overline{I}, P_{\mathrm{WT}}, N_{\mathrm{WT}}, D_{\mathrm{WT}}, A_{\mathrm{WPP}}) \tag{1}$$

A database of 1000 statistically representative WPP is generated to cover the variation observed in the European installed fleet of the WPP parameters ($\overline{I}, P_{\mathrm{WT}}, N_{\mathrm{WT}}, D_{\mathrm{WT}}, A_{\mathrm{WPP}}$). For each WPP, 10 different layouts are obtained using a space filling algorithm that maximizes the turbine spacing within the plant area. Wake losses as a function of wind speed are then computed for the 10 layouts at various wind directions using the Bastankhah Gaussian wake model [30] available in pywake [31]. This wake model consists of a Gaussian wind speed deficit, with linear wake expansion and a squared-sum wake superposition. To generalize the wind direction and layout dependencies in the wake losses, an average wake loss over the layouts and wind directions is used producing a database of wind speed dependent wake loss factors for each of the generic WPPs.

Using the database of wake loss factors and the generic WPP characteristics ($\overline{I}, P_{\mathrm{WT}}, N_{\mathrm{WT}}, D_{\mathrm{WT}}, A_{\mathrm{WPP}}$), an artificial neural network (ANN) with 7 hidden layers is trained. The performance of the resulting ANN is then validated on wake loss factors computed for actual WPPs in Europe. Details of the ANN architecture selection along with the results of the validation can be found in [32].

3.4. Wind generation and aggregation

WPP wind generation is obtained by interpolating the wake affected wind plant power curve at the wind speed for every time step. Note that the WPP database used in this article [22], includes a database of power curves of the turbines installed in Europe. A WPP efficiency of 0.95 is assumed for all plants, which includes 0.97 for availability and 0.98 of electrical and additional losses, as reported in [33]. Finally, the individual WPP generation time-series are aggregated into a country-level standardized generation time-series.

4. Validation metrics

Traditional validation metrics are used for comparing the observed (subscript O) and modeled (subscript M) time series such as: (1) bias or error of the mean ($e_{\overline{y}} = \overline{y}_M - \overline{y}_O$), (2) mean absolute error, MAE, (3) square root of the mean squared error, RMSE, and (4) sample or prediction correlation coefficient $r_y = \rho(y_M, y_O)$. Here, and in the following error metric definitions, y represents either the wind speed at a location (u) or the standardized wind generation of a country (P).

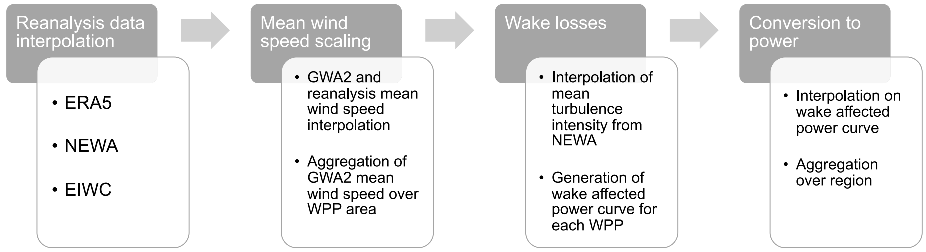

Fig. 3. Simulation model chain. Mean wind speed scaling is omitted for some models.

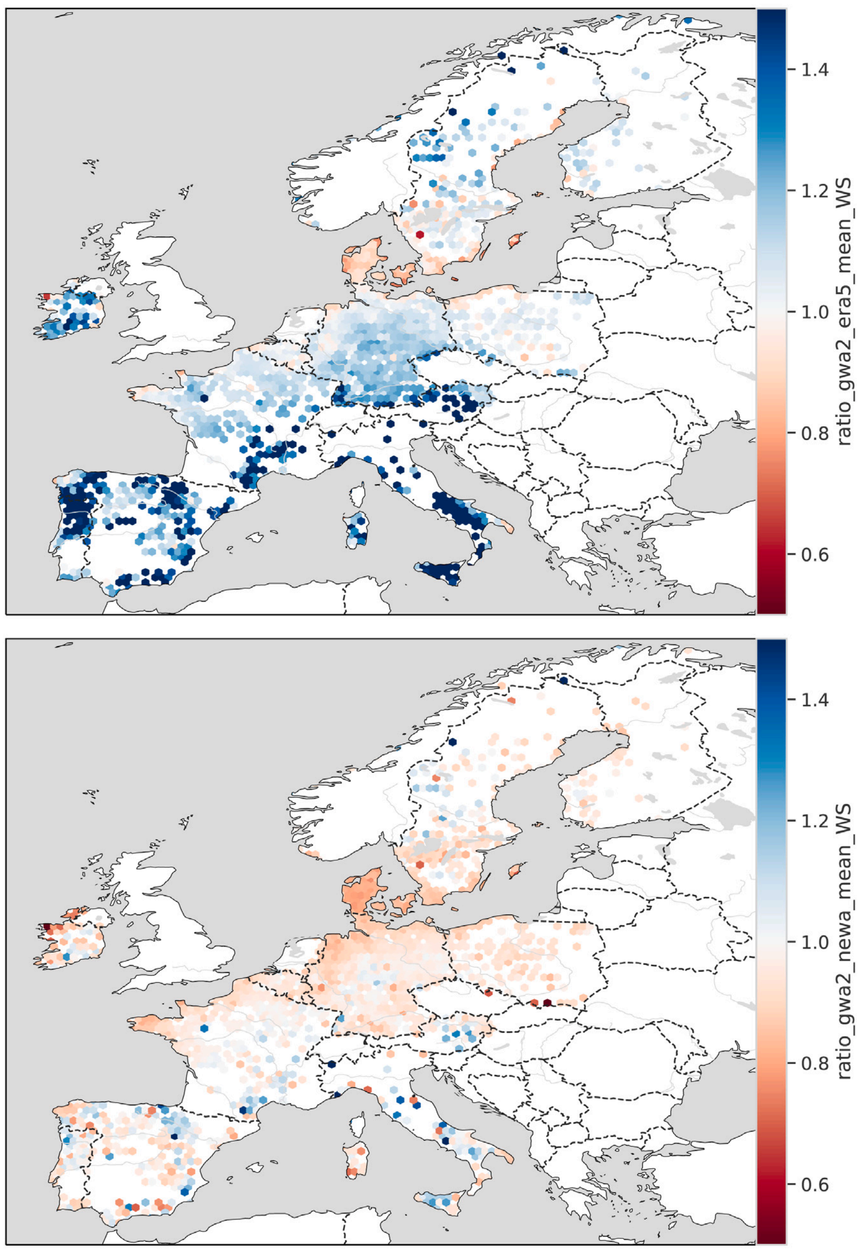

Fig. 4. Ratio between the mean wind speeds at the locations of the 2018 WPP installations: (top) $\overline{u}_{\text{GWA2}}/\overline{u}_{\text{ERA5}}$ (bottom) $\overline{u}_{\text{GWA2}}/\overline{u}_{\text{NEWA}}$.

4.1. New error metrics

This article introduces several new error metrics for wind speed or country-level wind generation time-series validation. The first error metric diagnoses diurnal cycle errors and is the error in the normalized mean wind speed at each hour on each month ($\overline{u}_{MD}$) over the mean wind speed, or the equivalent for standardized generation ($\overline{P}_{MD}$):

$$e_{\overline{y}\,MD} = \left(\frac{\overline{y}_{MD}}{\overline{y}}\right)_M - \left(\frac{\overline{y}_{MD}}{\overline{y}}\right)_O \tag{2}$$

Table 4
Wind speed distribution error metric statistics across all sites. Bold text indicates the best performing model per metric.

Model	$e_{\bar{u}}$		MAE_u		$RMSE_u$		r_u		$e_{u_{MD}} \times 10^3$		e_{F_u}	
	Mean	Std	Mean	Std	Mean	Std	Mean	Std	Mean	Std	Mean	Std
ERA5	**−0.06**	0.87	1.34	0.38	1.73	0.42	0.92	0.03	1.35	4.71	0.68	0.60
EIWR	0.30	0.73	1.94	0.26	2.55	0.30	0.80	0.04	**0.40**	**3.13**	0.61	0.56
NEWA	0.14	0.69	1.68	0.26	2.22	0.29	0.85	0.04	1.01	5.89	**0.52**	0.54
ERA5_GWA2	−0.36	**0.56**	**1.25**	0.19	**1.63**	**0.22**	**0.92**	**0.03**	1.35	4.71	0.60	0.37
EIWR_GWA2	−0.37	0.57	1.86	0.24	2.44	0.31	0.80	0.04	**0.40**	**3.13**	0.65	**0.35**
NEWA_GWA2	−0.35	0.56	1.63	**0.18**	2.16	0.23	0.85	0.04	1.01	5.89	0.61	0.36

The second metric quantifies the difference between the modeled and measured distributions of wind speed or wind generation. It consists in computing the area between the cumulative density functions ($F(x)$), note that this error metric is only positive and will take the value of the error of the mean if there is a bias in two equally distributed time series, for more information refer to [19]:

$$e_{F\,y} = \int_0^{\infty} |F(y_M) - F(y_O)|\, dy \tag{3}$$

Four additional validation metrics are used for comparing the time-series properties. Two metrics are used to compare the auto-correlation functions on a given location (x) or of a single country (x): one metric focuses on the auto-correlation function errors for 1 h lag:

$$e_{y_1} = \rho\,(\,y(x,t), y(x,t+1)\,)_M - \rho\,(\,y(x,t), y(x,t+1)\,)_O \tag{4}$$

while the other metric computes the mean of the errors in the auto-correlation function between 1 and N_l hours lag:

$$e_{y_{N_l}} = \frac{1}{N_l}\sum_{i=1}^{N_l} \rho\,(\,y(t), y(t+i)\,)_M - \rho\,(\,y(t), y(t+i)\,)_O \tag{5}$$

The last two metrics quantify the errors in the correlations of a point pair (x_i, x_j) (or country pair). The first error metric consists in computing the mean error in the spatial-correlation:

$$e_{X_y} = \frac{2}{N_l(N_l-1)}\sum_i \sum_{j<i} \rho\left(\,y(x_i,t), y(x_j,t)\,\right)_M - \rho\left(\,y(x_i,t), y(x_j,t)\,\right)_O \tag{6}$$

while the last error metric computes the error in the correlation of one hour ramps, $\Delta y(x,t) = y(x,t+1) - y(x,t)$ between two points or two countries:

$$e_{X_{\Delta y}} = \frac{2}{N_l(N_l-1)}\sum_i \sum_{j<i} \rho\left(\,\Delta y(x_i,t), \Delta y(x_j,t)\,\right)_M - \rho\left(\,\Delta y(x_i,t), \Delta y(x_j,t)\,\right)_O . \tag{7}$$

Finally, in order to characterize the spatial-correlation from each data set a characteristic length (L) is computed by fitting the following correlation to distance model, see Eq. (8); [34] presents several additional spatial-correlation models. Here the correlation between either a pair point wind speeds or 1h wind speed ramps is noted as ρ_{ij}, while the distance between the points is d_{ij}. The length scale is the distance in which the correlation takes a value of $1/e$, or using the fitted coefficients: $L = \alpha^{-1/\beta}$.

$$\rho_{ij} = \exp(-\alpha\, d_{ij}^{\beta}) \tag{8}$$

5. Results

5.1. Wind speed

An example of the simulated wind speed time-series is presented in Fig. 5. All the simulations capture the larger scale trends in the wind speed, but fail to capture the specific times in which wind speed fluctuations occur. This is a well know behavior of such data sets [35].

The overall results of the validation of the wind speed simulations are presented in Tables 4 and 5, The mean and standard deviation across all sites are also reported for every error metric and model in the tables. Fig. 6 shows the model versus measurements for the relevant variables used in the definition of error metrics focused on the wind speed distribution. The bias in the mean wind speed is smaller for ERA5 and NEWA than for the mean wind speed scaled models. However, the standard deviation of the errors (or the model uncertainty) are smaller for the GWA-scaled models than for using reanalysis data sets directly. The wind speed measurement locations cover mostly offshore and coastal areas; thus, the results can be expected to vary if more onshore wind speed measurement locations would be added to the analysis. ERA5 with GWA scaling (ERA5_GWA2) has the best traditional error metrics over all models, lowest mean MAE, lowest mean and standard deviation of RMSE, and the highest mean prediction correlation values with its lowest standard deviation across locations. NEWA_GWA2 has the lowest standard deviation of MAE across sites, with a value very close to ERA5_GWA2. EIWR has the lowest mean and standard deviation of errors in the normalized diurnal cycle, see Fig. 6 center. Nevertheless, all models show the same order of magnitude in accuracy to predict the normalized diurnal cycle with errors in the order of 10^{-3}. This means that all models capture reasonably well the diurnal and seasonal variability over the mean wind speed conditions. Note that GWA2 scaled models are omitted in the daily cycle figure as they provide the same normalized diurnal cycles results as the non-scaled models. NEWA has the lowest mean e_{F_u}, while EIWR_GWA2 has its lowest standard deviation across sites; but in general, all models show similar mean error in wind speed distribution over all the sites, while the standard deviation over all sites are lower for the models with mean wind speed scaling. This means that the mean wind speed scaling does improve the model accuracy to predict the wind speed distribution at a site.

Table 5
Wind speed time-series error metric statistics across all sites. Bold text indicates the best performing model per metric.

Model	e_{u_1}		$e_{u_{10}}$		e_{X_u}		$e_{X_{\Delta u}}$	
	Mean	Std	Mean	Std	Mean	Std	Mean	Std
ERA5	0.034	0.015	0.053	0.026	0.062	0.050	0.074	0.122
EIWR	0.029	0.014	**0.032**	0.019	**0.038**	0.052	0.042	0.074
NEWA	**0.018**	**0.012**	0.034	**0.018**	0.048	**0.046**	**0.010**	**0.025**

Auto-correlation error metrics are presented in Table 5 and visualized in Fig. 7 for some example sites and the overall wind speed auto-correlation model versus measurements (for aligned lags) for all sites. All models over-predict the auto-correlations, with the models with lower horizontal resolution having larger errors: ERA5, followed by EIWR and NEWA. Note that the GWA-scaled models are omitted as the correlation is the same as the non-scaled version of the model.

The spatial-correlations over distances for all sites are presented in Fig. 8, as well as the characteristic length of the correlation to distance model fit. Table 5 presents the mean and standard deviation of the different error metrics across all sites. All models are able to capture the spatial-correlation of wind speeds with small over-estimation of correlations of the order of 3%–6%. The characteristic length scale of the wind speed spatial-correlation for all models tends to be larger than the one estimated from the measurements, 13% for EIWR, 17% for NEWA and 21% for ERA5. The spatial-correlation of 1 h ramps of wind speed

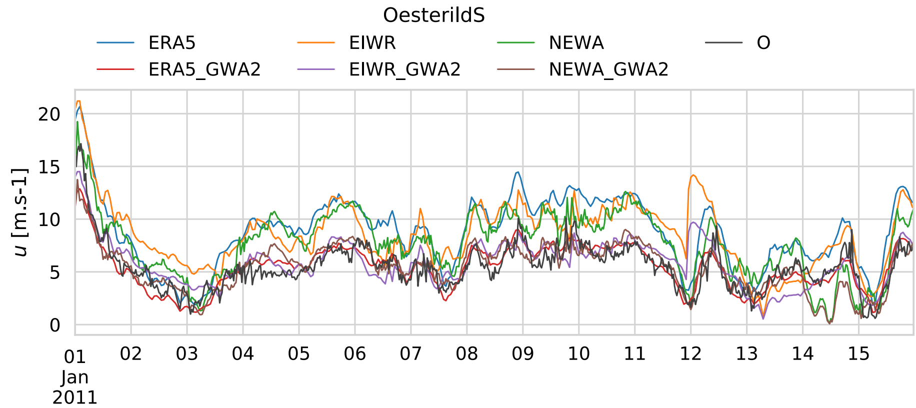

Fig. 5. Example wind speed time series for January 2011 at Østerild in the observations (O) and various reanalyses.

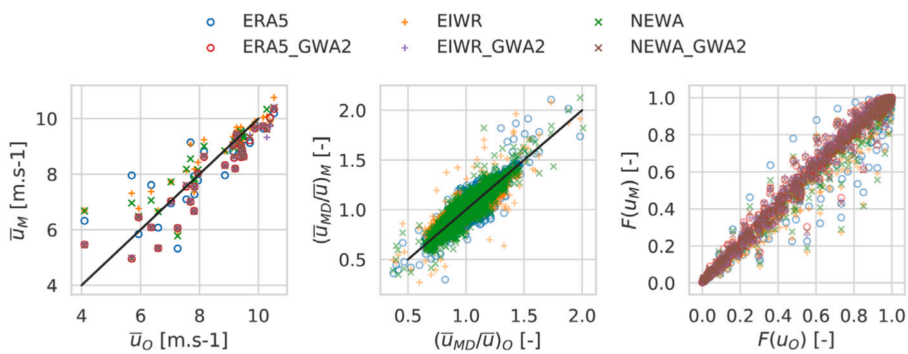

Fig. 6. Model (M) versus measurements (O) scatter plots: (left) mean wind speed, (center) mean wind speed at hour per month normalized by mean wind speed, (right) cumulative density function of the wind speed at specific values of [1, 2, …,25] [m s^{-1}].

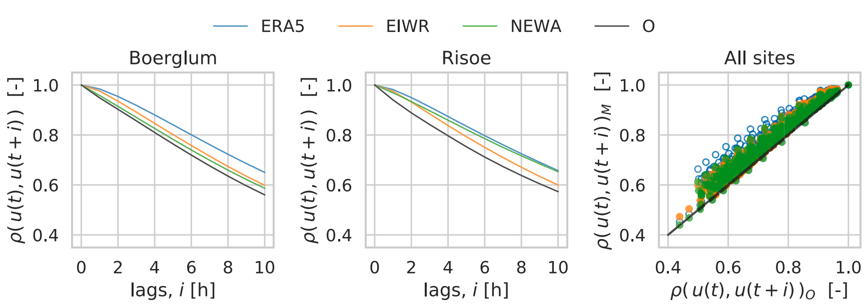

Fig. 7. Model and observations (O) wind speed auto-correlation for two example locations (left and center), and overall model versus measured auto-correlations at the same lags for all sites.

are better modeled by NEWA, while ERA5 largely over-estimates the spatial-correlations of 1 h ramps over all distances. The characteristic length scale of the 1 h ramp wind speed spatial-correlation is largely overestimated by the models.

5.2. Wind energy generation

An example of the country-level generation time-series is presented in Fig. 9. All the simulations capture the larger scale trends in the wind generation, but the GWA-scaled models tend to better follow the observed production.

Tables 6 and 7 present the overall results of the validation of the country-level wind generation statistics, while Fig. 10 depicts the model versus measurements for the relevant variable used in the definition of the different error metrics. The bias and standard deviation of errors in the capacity factor (mean standardized power) are smaller for the GWA-scaled models. Even though the distribution of prediction error for the capacity factors seems widely spread, the bias in CF is within 0.01–0.02. Individual country generation distributions are presented in the appendix in Fig. A.13. ERA5_GWA2 is consistently the best performing model in terms of mean and standard deviation across countries for MAE, RMSE and prediction correlation. Individual country-level prediction correlations are reported in the appendix in Table A.8.

All models show similar mean errors for predicting the diurnal cycle of generation in the order of 0.4×10^{-2}, while GWA2 scaled reanalyses have a slightly lower standard deviations of around 0.3×10^{-2}. This indicates that improvements need to be done in the time dependent wind-to-power transformation to reach the same accuracy levels seen in the wind speed diurnal cycle. ERA5 shows the largest deviations over multiple countries which demonstrates the need for mesoscale/microscale modeling. All the GWA2 scaled models show lower mean e_{F_u} error metric and standard deviations compared to using the reanalysis data directly.

The mean and standard deviation of the different error metrics across all countries for auto-correlation and spatial-correlation of the

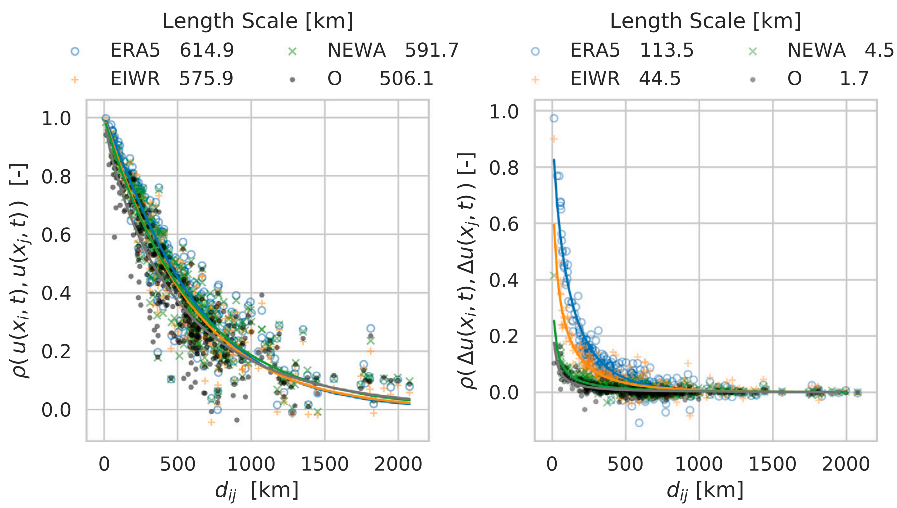

Fig. 8. (left) Measurement (O) and model wind speed spatial-correlation versus distance. (right) Measurement and model 1 h wind speed ramp spatial-correlation versus distance.

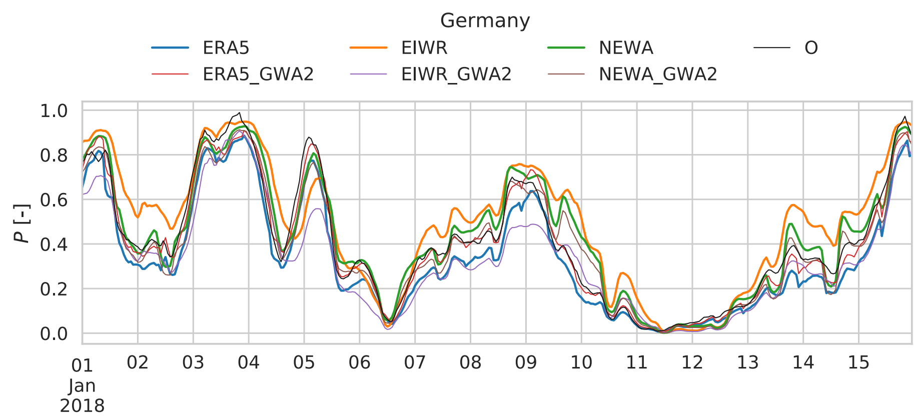

Fig. 9. Example of normalized wind energy generation time series for January 2018 aggregated for all Germany.

Table 6
Normalized wind power distribution error metric statistics across all countries. Bold text indicates the best performing model per metric.

Model	$e_{\overline{P}}$		MAE_P		RMSE_P		r_P		$e_{P_{MD}} \times 10^2$		e_{F_P}	
	Mean	Std	Mean	Std	Mean	Std	Mean	Std	Mean	Std	Mean	Std
ERA5	−0.05	0.07	0.08	0.04	0.10	0.05	0.94	0.04	0.26	0.60	0.07	0.05
EIWR	0.12	0.04	0.14	0.03	0.17	0.04	0.87	0.06	−0.41	**0.34**	0.12	0.04
NEWA	0.06	0.03	0.08	0.03	0.11	0.03	0.93	0.04	**−0.00**	0.40	0.06	0.03
ERA5_GWA2	0.02	0.03	**0.05**	**0.02**	**0.07**	**0.02**	**0.96**	**0.03**	0.09	0.35	0.03	0.02
EIWR_GWA2	**0.01**	**0.03**	0.07	0.02	0.10	0.03	0.89	0.05	−0.31	0.36	**0.03**	**0.02**
NEWA_GWA2	0.02	0.03	0.06	0.02	0.09	0.02	0.93	0.03	0.04	0.39	0.03	0.02

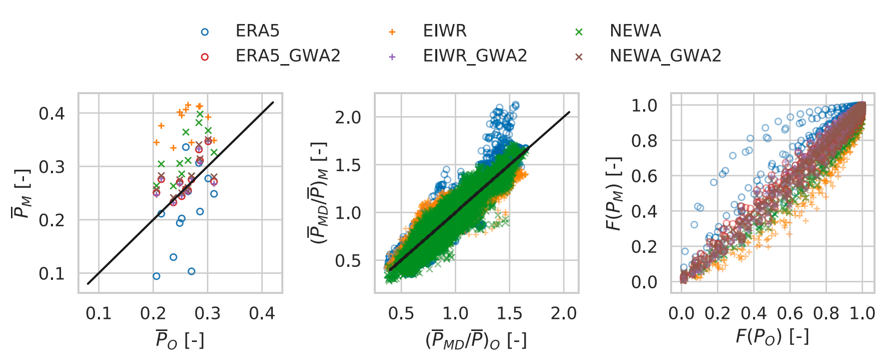

Fig. 10. Model versus measurements: capacity factor or mean standardized power (left), mean standardized power at hour per month normalized by mean standardized power (center), and cumulative density function of the standardized power at specific values [0, 0.125, …,1] (right).

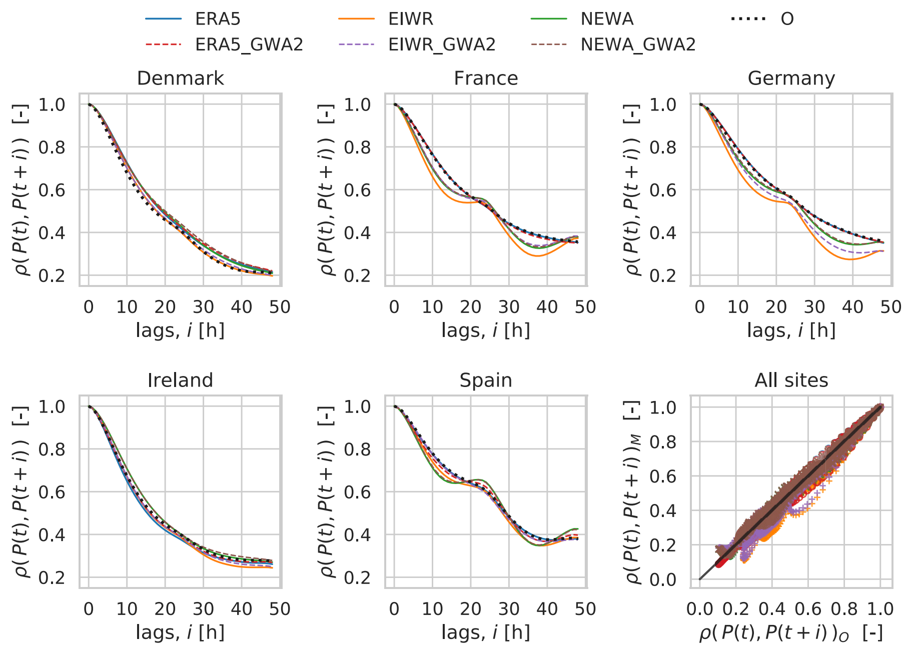

Fig. 11. Measurement and model wind speed auto-correlation for three individual countries (Denmark, France and Germany, Ireland and Spain), and overall for all sites.

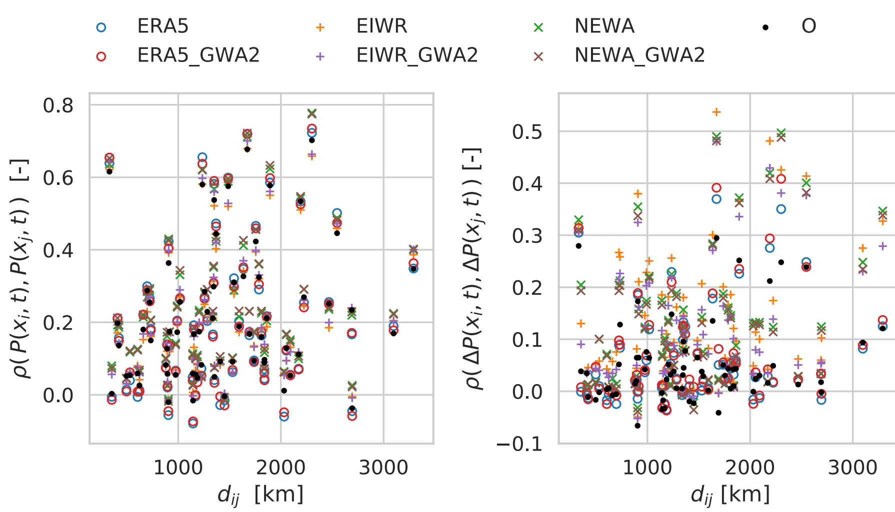

Fig. 12. (left) Measurement (O) and model country-level normalized wind generation spatial-correlation versus distance. (right) Measurement and model country-level normalized wind generation 1 h ramp spatial-correlation versus distance.

country-level wind generation simulations are presented in Table 7. There is no clear over-all best performing model in terms of auto- and cross-correlations. All models have small bias in the auto-correlation metrics, while the standard deviations tend to decrease for the GWA2 scaled models. All models are able to capture the spatial-correlation of wind generation (and its 1 h ramps) on the country-level, but GWA2 scaled models show similar across-site standard deviation of spatial-correlation errors as their correspondent non-scaled model (see Fig. 12).

Fig. 11 presents example auto-correlation functions and the over all model versus measurement auto-correlation plot. NEWA and EIWR (both models that use WRF) show growing errors with a 24 h periodicity, which indicates that there is a drifting trend from the boundary conditions given by the ERA5 or ERA-Interim reanalyses.

6. Discussion

As expected from previous studies [10,13], the errors in the prediction of mean wind speed are unbiased with WRF without microscale downscaling. On the contrary, the microscale mean wind speed scaling is necessary to decrease the uncertainty in the prediction of mean wind speed (standard deviation of mean wind speed errors) and to obtain an unbiased predictions of the country-level capacity factor. The over-prediction of mean wind speeds by NEWA in northern Europe is not reported in other studies [10,19]; however, this can be due to the lack of reliable validation data onshore in Denmark and Germany (two countries with the largest installed capacities). Nevertheless, other authors have reported a similar trend of over-prediction of mean wind speeds in Northern Europe and under-prediction of mean wind speeds in southern Europe [9,36], see Fig. 4.

The obtained prediction correlation with ERA5_GWA2 is larger than the ones reported in the literature with the previous generation reanalyses [11] and similar to the studies that rely on calibrating the generation distribution using the measurements [9]. For example, the prediction correlation of ERA5_GWA2 standardized wind generation (r_P) for Germany in this study is .984, while it is .981 in [9] or .97-.985 in [11]; for Spain r_P is .962 in this study while it is .917 in [11];

Table 7
Normalized wind power time-series error metric statistics across all countries. Bold text indicates the best performing model per metric.

Model	$e_{P_1} \times 100$		$e_{P_{10}} \times 100$		$e_{X_P} \times 100$		$e_{X_{\Delta P}} \times 100$	
	Mean	Std	Mean	Std	Mean	Std	Mean	Std
ERA5	0.02	0.25	−1.08	2.04	−0.34	3.46	**0.77**	**3.57**
EIWR	−0.08	0.32	−3.43	3.50	**−0.13**	3.01	9.35	6.52
NEWA	−0.04	0.22	**−0.09**	2.03	3.18	3.29	7.67	6.92
ERA5_GWA2	**0.00**	0.31	−0.87	**1.96**	−0.51	3.13	1.44	4.08
EIWR_GWA2	0.06	0.28	−2.25	3.25	0.70	**2.65**	6.82	5.22
NEWA_GWA2	**−0.00**	**0.21**	0.28	1.97	3.52	3.07	6.97	6.77

for France r_P it is .983 in this study while it is 0.976-.986 using high resolution regional reanalyses in [13]. This shows that ERA5 with a mean wind speed scaling (GWA2) and a simple wake modeling can achieve similar accuracy levels as those models that rely in the use of measured generation for calibration or high resolution reanalyses. The present bottom-up approach has the advantages of not needing measurements and being applicable for varying future wind installations without modifications, while the top-down approach needs to assume that the transfer function calibrated on an specific installation capacity will be the same in future fleets. The main disadvantage of the present approach is the high requirements on the technical data of the WT and WPP, even more WPP technical information is needed in comparison to [11] due to the wake modeling. The prediction correlation for Portugal for ERA5-based models is significantly lower compared to the other countries and compared to other models; the reasons for this should be investigated in future work.

We chose not to apply a Gaussian filtering of the single turbine power curve as done in [9,13] because the inclusion of wake and plant shutdown modeling are able to capture the distributions of country-level power production. Furthermore, we did not apply age dependent losses as suggested by [37] but instead used a total efficiency of 0.95. Age-dependent losses were considered, but applying them did not provide additional accuracy, so they were not applied.

This paper might provide an explanation to the results presented in [13] in terms of NEWA incorrectly simulating the wind speed daily cycle. NEWA shows a periodic discrepancy in the wind generation auto-correlation with respect the measurements with a 24 h period. This indicates that there are problems in the daily cycles in France and Germany even though NEWA has no bias and a similar model uncertainty in predicting the relative daily cycle of wind as the other data sets studied, including ERA5.

Larger standard deviation errors in generation diurnal cycle than wind speed diurnal cycle indicates that future improvements can be achieved by implementing a more accurate wind-to-power transformation. Time varying wake losses driven by the stability time series available in the different reanalysis data sets might be the missing diurnal-seasonal component of the generation.

We demonstrate that it is possible to accurately simulate large-scale regional wind energy generation using the GWA-scaled ERA5 data set and a generic wake model; here accuracy is understood as being able to simulate the distribution of wind generation and to produce time-series that have the right auto-correlations and spatial-correlations. In the country-level aggregation, the high-frequency variability in the measurements is smoothed out and thus compares well to ERA5 in terms of the country-level auto- and spatial-correlation statistics. We highlight that ERA5 is available starting from 1950 up to nowadays with releases occurring in almost real-time, a significantly larger period than NEWA/EIWR. This coverage will enable extreme event studies such as power fluctuation in storms [6] or modeling of the influence of wind in power outtakes. Regarding wake modeling the authors plan to make a new generation generic surrogate model to consider wind direction as well as stability dependent wake losses as time-series.

There are several limitations with the GWA scaling approach as the micro-scale resource assessment used. The GWA2 downscaling relies on the linear flow model WAsP, which is known for over-predicting wind speeds in complex terrain [10]. The approach proposed in this paper is not sufficient to simulate individual plant wind generation because the mean wind speed scaling does not take into account the effects of terrain in the wind direction time-series. Also, detailed wake modeling will require knowledge of the turbine layout, which is not available, and time dependent wake losses that are driven by the atmospherically stability and turbulence time-series.

The temporal properties of the ERA5 time series are significantly worse than those from NEWA for the prediction of wind speeds at individual locations or WPPs. This is a well known problem: the resulting time-series from WRF or coarser reanalysis data set are too smooth in comparison to individual point measurements. Stochastic models based on experimental missing wind speed spectra can be applied to simulate the missing high frequency component of the wind speed and wind generation [38–40].

7. Conclusions

Even though there is still room for improvement in terms of resolution, the ERA5 reanalysis can successfully be used for simulating large-scale wind energy production with similar levels of accuracy as using higher resolution weather mesoscale modeling. However, this is only true if the mean wind speed bias is corrected based on a high resolution micro-scale modeling and if wake losses are considered, at least in an approximated way. The combination of ERA5 and the Global Wind Atlas (GWA) shows good agreement with measured country-level generation data. The presented bottom-up approach can achieve similar levels of prediction-correlation with the measured country-level wind generation than simulations that rely on a period of measurements for calibration.

Due to the reduced coverage of the mean wind speed validation locations, the mean wind speed error distribution presented in this paper is biased towards offshore sites, therefore it does not represent southern Europe sites. For the available wind speed validation data, ERA5 shows the lowest bias in mean wind speed measurements, while GWA scaled models show the lowest standard deviations for mean wind speeds and lower area between the observed and modeled wind speed cumulative density function, e_{F_u}. All models are able to capture the daily cycles over the months with similar levels of precision and accuracy. In terms of auto- and spatial-correlation, the New European Wind Atlas (NEWA) shows the best fits to measurements but as expected there is missing high frequency variability in all models.

CRediT authorship contribution statement

Juan Pablo Murcia: Conceptualization, Methodology, Software, Validation, Formal analysis, Investigation, Data curation, Writing - original draft, Writing - review & editing, Visualization. **Matti Juhani Koivisto:** Conceptualization, Methodology, Writing - original draft, Writing - review & editing, Visualization, Supervision, Project administration. **Graziela Luzia:** Methodology, Formal analysis, Data curation, Writing - original draft, Visualization. **Bjarke T. Olsen:** Methodology, Formal analysis, Data curation, Software, Writing - original draft, Visualization. **Andrea N. Hahmann:** Writing - review & editing, Supervision, Project administration. **Poul Ejnar Sørensen:** Writing - review & editing, Supervision, Project administration. **Magnus Als:** Methodology, Formal analysis, Data curation, Software, Writing - original draft, Visualization.

Declaration of competing interest

The authors declare that they have no known competing financial interests or personal relationships that could have appeared to influence the work reported in this paper.

Acknowledgments

The authors would like to acknowledge "The Low-Wind turbine concept for optimal system integration" (Danish Energy Agency EUDP2019-I, Project number. 64019–0074), the ForskEL/EUDP OffshoreWake project (PSO-12521) and DTU Wind Energy PSfuture (La Cour Fellowship). The European Commission (EC) through FP7 (topic FP7-ENERGY.2013.10.1.2) and the Danish Energy Agency (EUDP 14-II, 64014–0590, Denmark) partly funded the NEWA project (New European Wind Atlas).

Appendix A. Individual country wind generation comparison

Individual country wind generation prediction correlations are presented for all models in Table A.8, while wind generation distribution are presented in Figs. A.13 and A.14 for the GWA2 scaled mean wind speed data sets, and the CF are reported. ERA5_GWA2 shows the best

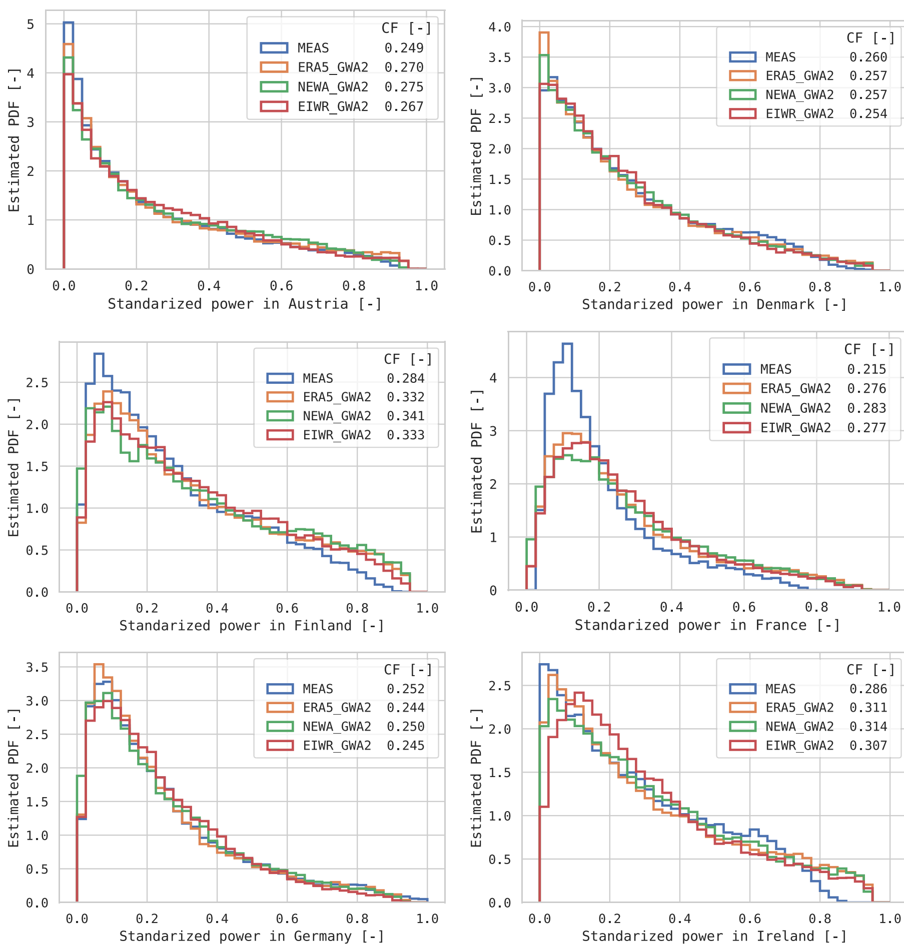

Fig. A.13. (First part) Distribution of normalized country-level generation for individual countries for GWA2 scaled models and for measurements (MEAS).

Table A.8
Prediction correlation r_P of standardized country-level generation for individual countries for all models.

	Austria	Denmark	Finland	France	Germany	Ireland	Italy	Norway	Poland	Portugal	Spain	Sweden
ERA5	0.934	0.970	0.954	**0.984**	0.984	0.935	0.896	0.920	0.977	0.830	0.926	0.960
EIWR	0.727	0.868	0.874	0.912	0.891	0.942	0.843	0.868	0.882	0.853	0.919	0.919
NEWA	0.826	0.934	0.917	0.945	0.954	0.948	0.912	0.903	0.947	**0.937**	0.932	0.953
ERA5_GWA2	**0.942**	**0.970**	**0.956**	0.983	**0.986**	**0.968**	**0.953**	**0.924**	**0.978**	0.880	**0.962**	**0.970**
EIWR_GWA2	0.756	0.882	0.884	0.941	0.927	0.935	0.850	0.870	0.911	0.854	0.911	0.921
NEWA_GWA2	0.831	0.939	0.921	0.949	0.958	0.945	0.913	0.906	0.951	0.937	0.933	0.955

results for almost all countries except Portugal and France. It can be observed that the distributions are well captured by all models for most countries. Specifically, south European countries (Italy, Portugal and Spain) tend to have larger errors as expected from the complex terrain of their wind installations, and are better modeled by ERA5-GWA2. Norway, Sweden and France tend to have larger errors than other countries, which could be due to less coverage or more errors in the technical data of installation database [7].

Appendix B. Wind speed measurements technical data

The technical data from the wind speed measurements including the respective heights used, time period, type of location and type of measurement device are listed in Table B.9. Anonymized stations were named according to the location: Northern North Sea (NNS), Central North Sea (CNS), South North Sea (SNS) and Western Baltic Sea (WBS).

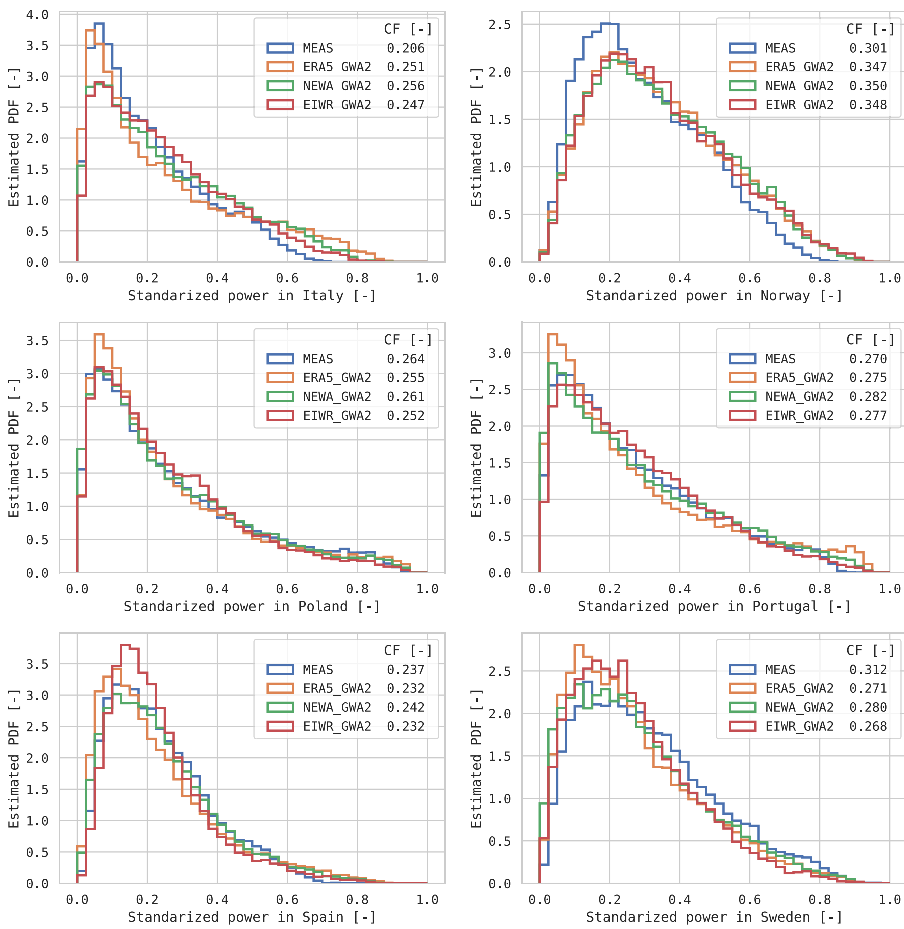

Fig. A.14. (continuation) Distribution of normalized country-level generation for individual countries for GWA2 scaled models and for measurements (MEAS).

Table B.9
Observational data sets. Type: meteorological masts (M), LIDAR (L); location: coastal (C); land (L); offshore (S); forest (F). Data sources: [a][41], [b][42], [c][43], [d][44], [e][45], [f][21], [g][46] and [h] commercial site. Availability [%] refers to the valid data within time coverage after the quality control.

Name	Height [m]	Time coverage	Availability [%]	Type	Location
Boerglum[a]	31.5	2006/06–2019/06	98.0	M	C
Cabauw[b]	140	2001/01–2018/12	99.8	M	L
CNS1[c]	108	2011/06–2012/05	93.6	L	S
CNS2[c]	70	2003/12–2009/12	87.7	M	S
CNS3[c]	102	2011/03–2012/05	71.0	L	S
CNS4[c]	105	2010/06–2011/07	37.8	L	S
CNS5[c]	106	2009/06–2011/08	84.3	L	S
DockingShoal[d]	90	2006/06–2013/04	87.5	M	C
FINO1[e]	90.3	2004/01–2018/12	87.8	M	S
FINO2[e]	92.4	2008/03–2017/11	91.1	M	S
FINO3[e]	90.5	2010/01–2018/11	91.1	M	S
GwyntYMor[d]	69	2000/09–2011/03	68.3	M	S
Hovsore[a]	100	2004/03–2019/03	97.6	M	C
Hyytiala[f]	67	1996/01–2003/08	91.4	M	F
Ijmuiden[g]	115	2012/01–2015/12	94.9	M	S
Lillgrund[a]	65	2009/01–2009/12	99.9	M	C
Lindenberg[f]	98	1999/01–2016/12	99.4	M	L
LondonArray[d]	82	2004/12–2011/12	70.7	M	S
NNS1[c]	105.5	2010/11–2011/11	88.4	L	S
NNS2[c]	100	2009/09–2011/09	59.6	L	S
Oesterild[a]	106	2015/02–2019/03	97.0	M	L
OesterildS[a]	44	2010/04–2011/09	95.6	M	L
Omoe[a]	50.6	2002/08–2005/06	96.7	M	C
Puijo[f]	75	2006/01–2015/12	94.4	M	L
Risoe[a]	125.2	2012/01–2019/03	99.4	M	L
Ryningsnaas[a]	138	2010/11–2012/02	92.1	M	F
SNS1[c]	116	2005/07–2010/12	83.2	M	S
SNS2[c]	72.5	2006/01–2010/07	98.2	M	S
SNS3[c]	110	2010/02–2011/03	85.9	L	S
Soroe[a]	43	2007/01–2011/11	87.6	M	F
Tystofte[a]	39	2000/01–2016/11	88.2	M	L
WBS1[h]	50	2006/06–2009/09	97.7	M	C

References

[1] IRENA. Global Renewables Outlook: Energy transformation 2050. Tech. rep., IRENA; 2020, URL https://www.irena.org/-/media/Files/IRENA/Agency/Publication/2020/Apr/IRENA_Global_Renewables_Outlook_2020.pdf.

[2] IEA. European Union 2020: Energy Policy Review. Tech. Rep., IEA; 2020, URL https://www.iea.org/reports/european-union-2020.

[3] Brown T, Schlachtberger D, Kies A, Schramm S, Greiner M. Synergies of sector coupling and transmission reinforcement in a cost-optimised, highly renewable European energy system. Energy 2018;160:720–39. http://dx.doi.org/10.1016/j.energy.2018.06.222.

[4] Gea-Bermúdez J, Pade LL, Koivisto MJ, Ravn H. Optimal generation and transmission development of the North Sea region: Impact of grid architecture and planning horizon. Energy 2020;191:116512. http://dx.doi.org/10.1016/j.energy.2019.116512.

[5] Crosara A, Tomasson E, Söder L. Generation adequacy in the Nordic and Baltic region: case studies from 2020 to 2050. Tech. rep., 2019, URL http://www.diva-portal.org/smash/record.jsf?pid=diva2:1336561.

[6] Murcia Leon J, Koivisto M, Sørensen P, Magnant P. Power fluctuations in high installation density offshore wind fleets. Wind Energy Science Discussions 2020;2020:1–23. http://dx.doi.org/10.5194/wes-2020-95.

[7] Koivisto M, Plakas K, Ellmann ERH, Davis N, Sørensen P. Application of microscale wind and detailed wind power plant data in large-scale wind generation simulations. Electr Power Syst Res190; 106638. http://dx.doi.org/10.1016/j.epsr.2020.106638.

[8] Cannon DJ, Brayshaw DJ, Methven J, Coker PJ, Lenaghan D. Using reanalysis data to quantify extreme wind power generation statistics: A 33 year case study in great britain. Renew Energy 2015;75:767–78. http://dx.doi.org/10.1016/j.renene.2014.10.024.

[9] Staffell I, Pfenninger S. Using bias-corrected reanalysis to simulate current and future wind power output. Energy 2016;114:1224–39. http://dx.doi.org/10.1016/j.energy.2016.08.068.

[10] Dörenkämper M, Olsen B, Witha B, Hahmann A, Davis N, Barcons J, Ezber Y, García-Bustamante E, González-Rouco J, Navarro J, Sastre-Marugán M, Sīle T, Trei W, Žagar M, Badger J, Gottschall J, Sanz Rodrigo J, Mann J. The making of the new European wind atlas – part 2: Production and evaluation. Geosci Model Dev 2020;13(10):5079–102. http://dx.doi.org/10.5194/gmd-13-5079-2020.

[11] Gonzalez-Aparicio I, Monforti F, Volker P, Zucker A, Careri F, Huld T, Badger J. Simulating European wind power generation applying statistical downscaling to reanalysis data. Appl Energy 2017;199:155–68. http://dx.doi.org/10.1016/j.apenergy.2017.04.066.

[12] Olauson J. ERA5: The new champion of wind power modelling? Renew Energy 2018;206:322–31. http://dx.doi.org/10.1016/j.renene.2018.03.056.

[13] Jourdier B. Evaluation of ERA5, MERRA-2, COSMO-REA6, NEWA and AROME to simulate wind power production over France. Adv Sci Res 2020;17:63–77. http://dx.doi.org/10.5194/asr-17-63-2020.

[14] Frank CW, Pospichal B, Wahl S, Keller JD, Hense A, Crewell S. The added value of high resolution regional reanalyses for wind power applications. Renew Energy 2020;148:1094–109. http://dx.doi.org/10.1016/j.renene.2019.09.138.

[15] Pickering B, Grams CM, Pfenninger S. Sub-national variability of wind power generation in complex terrain and its correlation with large-scale meteorology. Environ Res Lett 2020;15(4):044025. http://dx.doi.org/10.1088/1748-9326/ab70bd.

[16] Monforti F, Gonzalez-Aparicio I. Comparing the impact of uncertainties on technical and meteorological parameters in wind power time series modelling in the European union. Appl Energy 2017;206:439–50. http://dx.doi.org/10.1016/j.apenergy.2017.08.217.

[17] Hersbach H, Bell B, Berrisford P, Hirahara S, Horányi A, Muñoz Sabater J, Nicolas J, Peubey C, Radu R, Schepers D, et al. The ERA5 global reanalysis. Q J R Meteorol Soc 2020. http://dx.doi.org/10.1002/qj.3803.

[18] Nuño E, Maule P, Hahmann A, Cutululis N, Sørensen P, Karagali I. Simulation of transcontinental wind and solar PV generation time series. Renew Energy 2018;118:425–36. http://dx.doi.org/10.1016/j.renene.2017.11.039.

[19] Hahmann A, Sīle T, Witha B, Davis N, Dörenkämper M, Ezber Y, García-Bustamante E, González-Rouco J, Navarro J, Olsen B, Söderberg S. The making of the New European Wind Atlas – part 1: Model sensitivity. Geosci Model Dev 2020;13(10):5053–78. http://dx.doi.org/10.5194/gmd-13-5053-2020.

[20] Dee DP, Uppala SM, Simmons A, Berrisford P, Poli P, Kobayashi S, Andrae U, Balmaseda M, Balsamo G, Bauer dP, et al. The ERA-interim reanalysis: Configuration and performance of the data assimilation system. Q J R Meteorol Soc 2011;137(656):553–97. http://dx.doi.org/10.1002/qj.828.

[21] Ramon J, Lledó L, Pérez-Zanon N, Soret A, Doblas-Reyes FJ. The tall tower dataset: a unique initiative to boost wind energy research. Earth Syst. Sci. Data 2020;(12):429–39. http://dx.doi.org/10.5194/essd-12-429-2020.

[22] The wind power: Onshore wind farm database. 2019, URL https://thewindpower.net. [Accessed 15 Aug 2019].

[23] Erichsen G, Schülting O, Kather A. Making use of analytical wake models for large scale power system models by generation of generic efficiency fields. In: 18th wind integration workshop, October 16-18, 2019, Dublin. 2019, http://dx.doi.org/10.15480/882.2449.

[24] Open power system data. 2020. Data package time series. Version 2020-10-06. 2020, URL http://dx.doi.org/10.25832/time_series/2020-10-06. [Accessed 15 Nov 2020].

[25] IRENA Query tool. 2020, URL https://www.irena.org/Statistics/Download-Data. [Accessed 15 Nov 2020].

[26] ENTSO-E transparency platform. 2020, URL https://transparency.entsoe.eu. [Accessed 15 Nov 2020].

[27] Joos M, Staffell I. Short-term integration costs of variable renewable energy: Wind curtailment and balancing in Britain and Germany. Renew Sustain Energy Rev 2018;86:45–65. http://dx.doi.org/10.1016/j.rser.2018.01.009.

[28] EirGrid and SONI. Annual renewable energy constraint and curtailment report 2019. 2020, URL http://www.eirgridgroup.com/site-files/library/EirGrid/Annual-Renewable-Constraint-and-Curtailment-Report-2019-V1.2.pdf. [Accessed 1 Dec 2020].

[29] Gruber K, Klöckl C, Regner P, Baumgartner J, Schmidt J. Assessing the global wind atlas and local measurements for bias correction of wind power generation simulated from MERRA-2 in Brazil. Energy 2019;189:116212. http://dx.doi.org/10.1016/j.energy.2019.116212.

[30] Bastankhah M, Porté-Agel F. A new analytical model for wind-turbine wakes. Renew Energy 2014;70:116–23. http://dx.doi.org/10.1016/j.renene.2014.01.002.

[31] Pedersen MM, van der Laan P, Friis-Möller M, Rinker J, Réthoré P-E. DtuWindEnergy/PyWake: PyWake. 2019, http://dx.doi.org/10.5281/zenodo.2562662.

[32] Als ML. Generic wind farm wake losses for large scale simulations. (Master's thesis), Technical University of Denmark; 2020.

[33] Danish Energy Agency. Technology Catalogue, 2020. Tech. Rep., 2020, URL https://ens.dk/en/our-services/projections-and-models/technology-data/technology-data-generation-electricity-and. [Accessed 1st Feb 2020].

[34] Martin CMS, Lundquist JK, Handschy MA. Variability of interconnected wind plants: correlation length and its dependence on variability time scale. Environ Res Lett 2015;10(4):044004. http://dx.doi.org/10.1088/1748-9326/10/4/044004.

[35] Mehrens AR, Hahmann AN, Larsén XG, von Bremen L. Correlation and coherence of mesoscale wind speeds over the sea. Q J R Meteorol Soc 2016;142(701):3186–94. http://dx.doi.org/10.1002/qj.2900.

[36] Monforti F, Gonzalez-Aparicio I. Comparing the impact of uncertainties on technical and meteorological parameters in wind power time series modelling in the European union. Appl Energy 2017;206:439–50. http://dx.doi.org/10.1016/j.apenergy.2017.08.217.

[37] Staffell I, Green R. How does wind farm performance decline with age? Renew Energy 2014;66:775–86. http://dx.doi.org/10.1016/j.renene.2013.10.041.

[38] Larsén XG, Ott S, Badger J, Hahmann AN, Mann J. Recipes for correcting the impact of effective mesoscale resolution on the estimation of extreme winds. J Appl Meteorol Climatol 2012;51(3):521–33. http://dx.doi.org/10.1175/JAMC-D-11-090.1.

[39] Larsén XG, Larsen SrE, Petersen EL. Full-scale spectrum of boundary-layer winds. Bound-Lay Meteorol 2016;159(2):349–71. http://dx.doi.org/10.1007/s10546-016-0129-x.

[40] Koivisto M, Jónsdóttir GM, Sørensen P, Plakas K, Cutululis N. Combination of meteorological reanalysis data and stochastic simulation for modelling wind generation variability. Renew Energy 2020;159:991–9. http://dx.doi.org/10.1016/j.renene.2020.06.033.

[41] DTU. Technical university of Denmark - online data. 2020, URL http://rodeo.dtu.dk/rodeo/. [Accessed 15 Dec 2020].

[42] CESAR. Cabauw experimental site for atmospheric research. 2020, URL https://ruisdael-observatory.nl/cesar/. [Accessed 15 Dec 2020].

[43] Hasager CB, Stein D, Courtney M, na AP, Mikkelsen T, Stikland M, Oldroyd A. Hub height ocean winds over the North Sea observed by the NORSEWInD lidar array: Measuring techniques, quality control and data management. Remote Sens 2013;(5):4280–303. http://dx.doi.org/10.3390/rs5094280.

[44] Marine data exchange. 2020, URL http://www.marinedataexchange.co.uk/. [Accessed 15 Dec 2020].

[45] FINO – research platforms in the north sea and baltic sea. 2020, URL https://www.fino-offshore.de/en/. [Accessed 15 Dec 2020].

[46] Kalverla PC, Steeneveld G-J, Ronda RJ, Holtslag AA. An observational climatology of anomalous wind events at offshore meteomast IJmuiden (North Sea). J Wind Eng Ind Aerodyn 2017;(165):86–99. http://dx.doi.org/10.1016/j.jweia.2017.03.008.